The dynamics of tunneling into self-assembled InAs dots

R. J. Luyken, A. Lorke,[a] A. O. Govorov,[b] and J. P. Kotthaus
Sektion Physik/CeNS, LMU München, Geschwister-Scholl Platz 1, 80539 München, Germany

G. Medeiros-Ribeiro and P. M. Petroff
Department of Materials and QUEST, University of California, Santa Barbara, California 93106

(Received 11 November 1998; accepted for publication 20 February 1999)

Using frequency-dependent capacitance spectroscopy, the dynamics of tunneling into arrays of self-assembled InAs quantum dots is investigated with respect to sample geometry, Coulomb interaction, and magnetic field. An equivalent resistance-capacitance circuit is derived which allows us to determine the tunneling times for each state of the dots. The different tunneling times for different many-particle states are explained by a reduced tunneling barrier and Coulomb interaction. A magnetic field applied perpendicular to the tunneling direction results in a strong suppression of the charging signal, which is attributed to enhanced localization caused by the magnetic field. Calculations for three-dimensional to zero-dimensional magnetotunneling can account for the experimental data. © *1999 American Institute of Physics.* [S0003-6951(99)01217-6]

Recently, self-assembled strained islands have attracted particular attention as they provide for well-defined, nanometer-size quantum dots with sizes in the 10 nm range.[1] These systems are of great interest, not only for studying the basic properties of man-made ''artificial atoms,'' but also because of possible device applications. Using capacitance and far-infrared spectroscopy, the many-particle ground states and the excitations of the dots have been previously investigated in detail[2–4] as well as the optical properties of these promising candidates for improved laser design.[5]

Here, we investigate the dynamics of tunneling from a three-dimensional back contact into ensembles of self-assembled InAs quantum dots by frequency-dependent capacitance spectroscopy. Apart from the influence of the tunneling barrier thickness, we investigate here the influences of Coulomb blockade, magnetic fields, and temperature. Our investigations show that by suitable sample design the tunneling time can be adjusted in a wide range which promises technical applications ranging from charge storage to ultrafast switching.

The samples are grown by molecular beam epitaxy, using the Stranski–Krastanow growth to create the self-assembled InAs quantum dots. From atomic force micrographs of similarly grown samples, we estimate the InAs dots to be approximately 20 nm in diameter and 6 nm in height. The dots are embedded into a suitably designed GaAs/AlGaAs heterostructure[3,6] with a tunneling barrier of thickness d_1 and a blocking barrier of thickness d_2 [Fig. 1(a)]. Using the simple lever arm argument,[3] a voltage ΔV applied between the gate and the back contact can be converted approximately into an energy shift of the dots[7] $\Delta E = e\Delta V d_1/(d_1+d_2)$. The samples are provided with ohmic contacts and a semitransparent gate. The gate area is 0.2 mm^2 and thus with typical dot densities of $10^{10}/cm^2$, ensembles with approximately 2×10^7 dots are probed. The capacitance–voltage ($C-V$) spectra are measured at 4.2 K using a dual-phase lock-in amplifier.

As described in Refs. 2 and 3, the lowest and second-lowest single electron states of the InAs quantum dots are doubly and fourfold degenerate, respectively. For the many-particle states, this degeneracy is lifted by electron–electron interactions, so that groups of charging peaks appear, which, in analogy to atomic physics, are commonly labeled *s* and *p* shell.

Figure 1(b) shows $C-V$ traces of a structure with $d_1 = 40$ nm and $d_2 = 200$ nm at frequencies from 2 up to 400 kHz at $T = 4.2$ K. At first glance, it can already be seen that increasing the frequency affects the different states differently: the *s* states are strong, the *p* states are weaker, and the wetting layer is not affected at all in this frequency regime.[8] This can be explained qualitatively by the fact that an increase in gate voltage results in a decrease of the tunneling

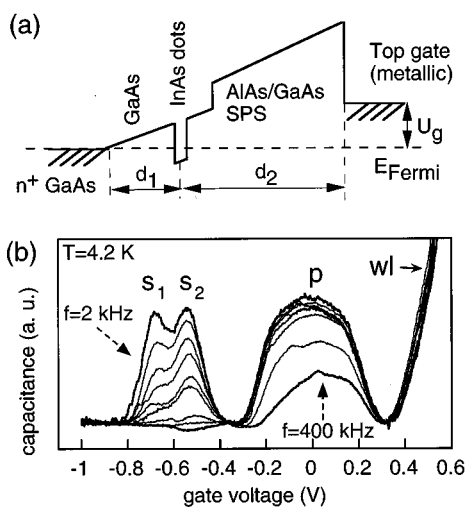

FIG. 1. (a) Sketch of the conduction band edge along the growth direction of the investigated sample. $d_1 = 40$ nm and $d_2 = 200$ nm. (b) Capacitance–voltage ($C-V$) traces recorded at frequencies 2.3, 8.3, 13.8, 20.1, 33, 43, 101, 200, and 400 kHz ($T = 4.2$ K). The background capacitance between the gate and the back contact has been subtracted.

[a]Electronic mail: Axel.Lorke@physik.uni-muenchen.de
[b]Permanent address: Institute of Semiconductor Physics, 630090, Novosibirsk, Russia.

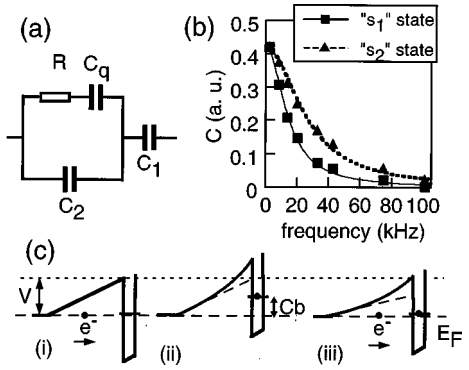

FIG. 2. (a) Equivalent RC circuit derived from the balance of charge. From the commonly used RC circuit it differs by the ''quantum capacitance'' C_q. (b) Capacitance amplitude of both s_1 and s_2 state plotted against frequency and fitted according to $I(t)=i\omega\Delta U e^{i\omega t}C_2[(C_1+C_q^*)/(C_1+C_2+C_q^*)]$. (c) The effect of Coulomb blockade on the tunneling barrier.

barriers heights. A more qualitative analysis is given below.

Assuming sufficiently low temperature, we describe the charge transfer between the dot layer and the back contact by a simple decay equation, with a decay tunneling time τ

$$\frac{dn_D}{dt}=-\frac{eD\Delta\mu}{\tau}=-\left(\frac{\Delta n_D-eD\Delta\phi}{\tau}\right). \tag{1}$$

Here, D is the density of states and n_D is the charge density in the dot layer. Its change in time (which is essentially the current going into the dot layer) is proportional to the difference in electrochemical potential[9] $\Delta\mu$ between the back contact and the dot layer. $\Delta\mu$ contains both a contribution from $\Delta\phi$, the potential drop between the back contact and the dot layer, and from Δn_D, the deviation from equilibrium of the charge in the dot. We assume that the applied voltage $U=U_0+\Delta U e^{i\omega t}$ induces a linear response in the sample. The current response of the sample (which is proportional to the measured capacitance signal) is given by $I(t)=d/dt(n_B+n_D)$. Using Eq. (1) and Gauss' law a straightforward calculation allows to write the current as a function of sample parameters:

$$I(t)=i\omega\Delta U e^{i\omega t}C_2\frac{C_1+C_q^*}{C_1+C_2+C_p^*} \tag{2}$$

with $C_1=\epsilon_0\epsilon/d_1$, $C_2=\epsilon_0\epsilon/d_2$, $C_q^*=C_q/(1+i\omega\tau)$, $C_q=e^2D$.

This is equivalent to a passive resistance-capacitance (RC) circuit as shown in Fig. 2(a) with $\tau=RC_q$. Note that this circuit has not been proposed *ad hoc* but has been derived from the balance of charge in the device. It differs by the additional ''quantum capacitance'' C_q from the commonly used RC circuit (Ref. 6 and references therein). The averaged charging time τ can be derived from fitting the measured capacitances to the imaginary part of Eq. (2) [Fig. 2(b)]. For the present sample with $d_1=40$ nm and $d_2=200$ nm, we obtain for the s_1 state a value of 496 μs, and 268 μs for the s_2 state. The different values of τ for the different states are a direct consequence of three-dimensional (3D) to zero dimensional (0D) tunneling, because the underlying physical mechanism is the Coulomb blockade.

The tunneling process from the back contact into the dot layer is modeled by sequential tunneling through a barrier with transmission coefficient T. In a first approximation, a triangular barrier for the tunneling into the s_1 state is assumed. Then the tunneling coefficient in WKB approximation is given by $T^2=\exp[-4d_1\sqrt{2m^*V}/(3\hbar)]$. With the effective mass of GaAs $m^*=0.0069m_e$, $d_1=40$ nm, and $V=180$ meV as the height of the tunneling barrier derived from optical experiments, we obtain a value of $T^2=9.3\times10^{-14}$. Although for a precise calculation of the tunneling time the simple triangular model is too crude,[10] it is able to explain the influence of the Coulomb blockade on the charging time of the two s states. For this, it must be considered how charge in the dot locally modifies the band structure. We assume the dot as a disk, homogeneously charged with a single electron and calculate its potential along the growth direction. This potential adds to the triangular potential as shown in Fig. 2(c) (ii) with the result of lifting the dot levels by the Coulomb blockade. With increasing gate voltage the one-electron ground state of the dot matches again with the Fermi energy and the dot is filled with the second electron [Fig. 2(c) (iii)]. Compared to the filling of the s_1 state [Fig. 2(c) (i)], the tunneling barrier for the s_2 state [Fig. 2(c) (iii)] is reduced. In WKB approximation, the transmission coefficients are calculated and from that the relation between the tunneling times for the two states. From this calculation, the resulting charging time of the s_2 state is reduced to 35% of the s_1 state compared to 52% obtained from the experimental evaluation. Given the exponential dependence of the transmission coefficient on both d_1 and V, we consider the agreement between theory and experiment satisfactory. For $V_{\text{eff}}=140$ meV and $d_{\text{eff}}=38$ nm (see below), the calculated charging time of the s_2 state is reduced to 32% of the s_1 state.

A variation of the length of the tunneling barrier, which can be easily done by the design of the structure, makes it possible to tune the charging time of the dots to a well-defined value in the range from below a few hertz to some gigahertz; already for samples with $d_1=25$ nm, we do not observe any frequency dependence up to a megahertz. Furthermore, with a ''slow'' tunneling process for the lowest (s states) and a ''fast'' tunneling time for the p states, a suitably applied electric pulse could raise the Fermi energy to the level of the p state before tunneling to the s state occurs. This offers the possibility to populate the p state, while the s state remains empty[11] and thus to achieve population inversion.

A possibility to tune the tunneling time τ *in situ* lies in the application of a magnetic field perpendicular to the tunneling path. Whereas it is known that this field orientation only marginally influences the dots' energy levels, it can drastically alter the charging dynamics. From Fig. 3(a) it can be seen that at fixed frequency, an increase in B field has qualitatively the same effect on the shape of the C–V trace as increasing the frequency in Fig. 1(b). The experimentally determined tunneling times for the s_1 state are shown in Fig. 3(b). Magnetic field effects in tunneling were previously considered for various semiconductor systems (e.g., Refs. 12 and references therein). We use the approach proposed in Refs. 13 to calculate the B dependence of τ. This method was used before to describe tunneling into traps in the semiconductor-dielectric system and in quantum

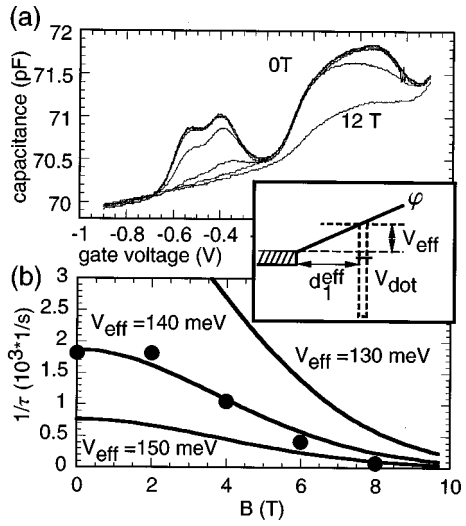

FIG. 3. (a) $C-V$ traces with magnetic fields applied parallel to the sample surface in 2T steps from 0 to 12 T ($T=4.2$ K, $f=2.3$ kHz). (b) Inverse tunneling times for the s_1 state at magnetic fields 0,2,4,6,8 T derived from the experiment (data points) compared to theoretical trace of $W(B)$ according to Eq. (3) with $V_{\text{eff}}=140$ meV, $d_1^{\text{eff}}=38$ nm. The calculated traces for $V_{\text{eff}}=130$ meV and $V_{\text{eff}}=150$ meV are also shown (solid lines). The inset shows schematically the potentials used in the model for 3D–0D magnetotunneling.

wells.[14] The probability of 3D–0D tunneling, $W=1/\tau$, is written as

$$W=\frac{2\pi}{\hbar}\sum_{\alpha}|\langle\Psi_{\alpha}|V_{\text{Dot}}|\Psi_0\rangle|^2\delta(E_{\alpha}-E_0), \tag{3}$$

where Ψ_0 and E_0 are the wave function localized in a quantum dot and its energy, respectively, Ψ_{α} and E_{α} are the wave functions of electrons in the back contact and their energies. The wave functions Ψ_{α} are calculated for the potential φ (see inset in Fig. 3) and exponentially decay in the barrier region. The wave function Ψ_0 is strongly localized in the quantum dot, so that neither the magnetic field nor the exact shape of φ essentially changes Ψ_0. The wave functions Ψ_{α} in the back contact (which is treated as a bulk electron plasma), however, are strongly affected by B. To calculate Ψ_{α}, we use a quasi-classical approach[15] and the vector potential in the form $A=(0,-B\cdot z,0)$. Here (x,y) and z are the in-plane and normal coordinates, respectively. The wave function of a quantum dot is modeled by $\Psi_0=\chi(z)\times(\sqrt{\pi}l_0)^{-1}\exp(-(x^2+y^2)/(2l_0^2))$, where $\chi(z)$ is the wave function in a square quantum well of width $L=4$ nm and depth 650 meV. The harmonic-oscillator function $\exp[-(x^2+y^2)/(2l_0^2)]$ describes the lateral motion in a quantum dot.[3] The length $l_0=\sqrt{\hbar/(m^*\omega_0)}$ with $\hbar\omega_0=50$ meV.[3] For the Fermi energy in the back contact, we take $E_F=100$ meV from a self-consistent modeling of the given layer structure. The best fit to the experiment assures for $V_{\text{eff}}=140$ meV and $d_1^{\text{eff}}=38$ nm. Figure 3(b) shows the calculated values of W as a function of the magnetic field compared to the experimental results. The value V_{eff} actually describes the effective height of the tunneling barrier. It can be somewhat less than the value from the optical data (180 meV) because strain will change the potential shape and result in an effectively lowered barrier height. The effective width of the barrier d_1 can be less than 40 nm at nonzero voltage V_{gate}. Thus, there is a qualitative agreement between theory and experiment.

In the low temperature regime, we observe only a moderate temperature dependence, e.g., decreasing the temperature from 4 K to 30 mK only enhances the tunneling time by a factor of 1.6. This justifies the $T=0$ K quantum mechanical treatment above.

In conclusion, we have shown that both a variation of the sample geometry and the application of a magnetic field can be used to tune the charging dynamics into self-assembled InAs quantum dots in a wide range, which promises attractive implementations in both nanoscale physics and possible single electron devices.[16]

The authors would like to acknowledge stimulating discussions with S. Manus and S. Ulloa. This work is supported by the BMBF via Grant No. 01BM623, by a Max-Planck research award, by QUEST, and by FOROPTO.

[1] L. Goldstein, F. Glas, J. Y. Marzin, M. N. Charasse, and G. LeRoux, Appl. Phys. Lett. **47**, 1099 (1985); D. Leonard, K. Pond, and P. M. Petroff, *ibid.* **63**, 3203 (1993); J. Y. Marzin, J. M. Gerard, A. Izrael, D. Barrier, and G. Bastard, Phys. Rev. Lett. **73**, 716 (1994).
[2] H. Drexler, D. Leonard, W. Hansen, J. P. Kotthaus, and P. M. Petroff, Phys. Rev. Lett. **73**, 2252 (1994).
[3] M. Fricke, A. Lorke, J. P. Kotthaus, G. Medeiros-Ribeiro, and P. M. Petroff, Europhys. Lett. **36**, 197 (1996); B. T. Miller, W. Hansen, S. Manus, R. J. Luyken, A. Lorke, J. P. Kotthaus, S. Huant, G. Medeiros-Ribeiro, and P. M. Petroff, Phys. Rev. B **56**, 6764 (1997).
[4] P. N. Brounkov, A. Polimeni, S. T. Stoddart, M. Henini, L. Eaves, P. C. Main, A. R. Kovsh, Y. G. Musikhin, and S. G. Konnikov, Appl. Phys. Lett. **73**, 1092 (1998).
[5] S. Fafard, K. Hinzer, S. Raymond, M. Dion, J. McCaffrey, and S. Charbonneau, Science **274**, 1350 (1996).
[6] G. Medeiros-Ribeiro, J. M. Garcia, and P. M. Petroff, Phys. Rev. B **56**, 3609 (1997).
[7] This linear lever arm picture is exact only as long as the dots are uncharged. However, simulations with a 1D-Poisson solver show that for the relevant charge densities, it is appropriate to use this argument for the calculation of the energy levels of the dots.
[8] The limitation is here the oscillator frequency of the lock-in amplifier. On samples with larger tunneling barrier d_1 both the p states and the wetting layer are (at sufficiently high frequencies) affected in the same way as here the s states.
[9] N. W. Ashcroft and N. D. Mermin, *Solid State Physics* (Saunders, Philadelphia, 1976).
[10] The effective distance between the dots and the back contact is slightly different from the geometric value due to a spreading of charge from the back contact. In addition, the strain field from the dot modifies the conduction band. See J. H. Davies, J. Appl. Phys. **84**, 1358 (1998).
[11] First indications for this effect can be observed as a difference between the charging and the decharging signal.
[12] A. H. Fertig and B. I. Halperin, Phys. Rev. B **36**, 7969 (1987).
[13] J. Bardeen, Phys. Rev. Lett. **6**, 57 (1961); E. O. Kane, in *Tunneling Phenomena in Solids*, edited by E. Burstein and S. Lundqvist (Plenum, New York, 1969).
[14] I. Lundström and C. Svensson, J. Appl. Phys. **43**, 5045 (1972); A. O. Govorov and W. Hansen, Phys. Rev. B **58**, 12980 (1998).
[15] L. D. Landau and E. M. Lifshitz, *Quantum Mechanics* (Pergamon, Oxford, 1975).
[16] K. K. Likharev, Appl. Phys. Lett. **73**, 2137 (1998).